Magnetic properties and magnetocaloric effect in thiospinel Fe1-Cu Cr2S4 (x = 0.0, 0.5) compounds

E. Choker, S. El Haber, F. Richomme, D. Pelloquin, A. Fnidiki, S. Hebert, Jean Juraszek

Magnetic properties and magnetocaloric effect in thiospinel $Fe_{1-x}Cu_xCr_2S_4$ (x = 0.0, 0.5) compounds

E. Choker[1], S. El Haber[2], F. Richomme[1], D. Pelloquin[2], A. Fnidiki[1], S. Hebert[2], J. Juraszek[1]

[1]Univ Rouen Normandie, INSA Rouen Normandie, CNRS, Normandie Univ, GPM UMR 6634, F-76000 Rouen, France

[2]Univ Caen Normandie, ENSICAEN, CNRS, Normandie Univ, CRISMAT UMR 6508, F-14000 Caen, France

Email : jean.juraszek@univ-rouen.fr

ABSTRACT

In this study, we investigate the magnetic and magnetocaloric properties of Cr-based spinel sulphides $Fe_{1-x}Cu_xCr_2S_4$ (x = 0.0 and x = 0.5). The magnetic transition temperature of $FeCr_2S_4$ (176 K) increases to 330 K when 50% of Fe in $FeCr_2S_4$ structure is substituted with Cu. Temperature-dependent Zero-Field-Cooled (ZFC) and Field-Cooled (FC) magnetic moment measurements show a paramagnetic (PM) to ferrimagnetic (FiM) phase transition in our samples. Magnetocaloric properties were investigated through magnetization isotherm measurements. The maximum magnetic entropy change values are -2.78 J/Kg. K and -2.11 J/Kg. K under 5 T magnetic field, for x = 0 and x = 0.5 in $Fe_{1-x}Cu_xCr_2S_4$, respectively. Analysis of phenomenological universal curves and Arrott plots indicate a second-order magnetic transition for both compounds. Consequently, $Fe_{0.5}Cu_{0.5}Cr_2S_4$ emerges as a promising candidate for magnetic refrigeration applications due to its considerable high magnetic entropy change and its proximity to room temperature transition.

Keywords Spinel coumpounds, Magnetocaloric effect, Magnetic entropy change, Relative cooling power.

1. Introduction

The Magnetocaloric Effect (MCE) is acknowledged as an interesting property intrinsic to all magnetic materials. Magnetic refrigeration based on MCE is advantageous due to its low

energy consumption and environmentally friendly characteristics, making it a promising alternative gas compression refrigeration technology [1, 2]. The magnetocaloric effect is associated with the magnetic entropy change $(-\Delta S_M)$, resulting from the coupling between the magnetic material sublattice and the external magnetic field $\mu_0 H$. In the presence of a magnetic field variation ΔH, the magnitude of $(-\Delta S_M)$ reaches its maximum peak in the vicinity of the magnetic phase transition temperatures T_c. A lot of magnetic materials with giant MCE and featuring a first-order magnetic transition have been studied [3-5]. However, the irreversibility behavior of their field and thermal magnetization limits their practical applications [6]. Typically, materials with a first-order magnetic transition are characterized by a narrow and sharp peak in magnetic entropy changes $(-\Delta S_M)$ around the transition temperature. This is in contrast to second-order magnetic transition (SOMT), which implies a very large magnetic entropy change $(-\Delta S_M)$ [7, 8]. Despite this, SOMT materials exhibit a significantly high Relative Cooling Power (RCP) and favorable reversible magnetic behavior [9]. Therefore, SOMT materials are recognized as key factors for achieving high efficiency in magnetic refrigeration.

In recent years, transition metal spinel structures with the general formula AB_2S_4, have attracted considerable attention due to their versatile physical properties. Specifically, the ferrimagnetic spinel structure $Fe_{1-x}Cu_xCr_2S_4$ ($0 \leq x \leq 1$) has attracted significant attention due to its fascinating electronic and magnetic properties, including colossal negative magnetoresistance and semiconducting behavior [10]. In these structures, chalcogen anions form a close-packed face-centred cubic lattice, with divalent A^{2+} ions occupying 1/8 of the tetrahedral sites, and trivalent B^{3+} occupying 1/2 of the octahedral sites. The magnetism in spinel materials arises from the partially filled d-orbitals of transition metals. In $FeCr_2S_4$, magnetic Fe^{2+} ($3d^6$, S=2) ions occupy the tetrahedral A-sites, while magnetic Cr^{3+} ($3d^3$, S=3/2) ions reside in the octahedral B-sites [11]. The spin magnetic moments of Fe and Cr ions couple ferromagnetically among themselves, but couple antiferromagnetically with each other. $FeCr_2S_4$ exhibits a Curie temperature T_c in the range of 165-180 K [10], [12, 13]. Recent studies show that the magnetic transition temperature increases when Fe is substituted by Cu in the tetrahedral A-sites [14, 15]. In $Fe_{0.5}Cu_{0.5}Cr_2S_4$, the magnetic transition temperature shifts close to room temperature [16, 17]. This adjustment makes $Fe_{0.5}Cu_{0.5}Cr_2S_4$ particularly significant

for practical applications at room temperature, emphasizing its potential as a highly promising material for advanced technological applications including magnetic refrigeration.

In the present work, we will focus on the ferrimagnetic spinel $Fe_{1-x}Cu_xCr_2S_4$ (x = 0.0, x = 0.5) compounds. Our investigation will encompass an in-depth analysis of magnetic properties, particularly the exploration of magnetic entropy changes. We have reported a notable magnetic entropy change around their Curie temperatures T_c under an applied field variation of $\Delta H = 5$ T. These results suggest that the thiospinel compounds are promising candidates for use as working materials in magnetic refrigeration technology.

2. Experimental details:

Polycrystalline samples $Fe_{1-x}Cu_xCr_2S_4$ (x = 0.0, x = 0.5) were synthesized by solid-state reactions of Fe, Cu, Cr, and S in a controlled environment inside a dry glove box. A total of 1 gram was weighed, following the stoichiometric ratio of the $FeCr_2S_4$ and $Fe_{0.5}Cu_{0.5}Cr_2S_4$ formulas. After mixing by grinding in an agate mortar, the powder was pressed into bars (2 × 2 × 10 mm), which were sealed into a quartz tube under vacuum. The sealed tube underwent thermal treatment at 800°C for 12 hours. After this initial heating, the obtained bars were ground into powder for a second round of heat treatment, following a similar process. X-ray powder diffraction (XRPD) was performed at room temperature using a Panalytical X-Pert Pro diffractometer with cobalt radiation (Co-K_α = 1.7886Å/1.7929Å) and equipped with an X'Celerator detector. The X'pert Highscore Plus suite was used to check the purity and identify the possible secondary phases. Structure refinement was conducted using the Rietveld method based on the FullProf program implemented in the WinPLOTR Suite [18]. The magnetization data were collected via conventional zero-field-cooled (ZFC) and field-cooled (FC) modes under an applied induction field of 0.01 T. Data were collected during the heating process (ZFC curve) and subsequently during cooling back to 5 K (FC curve). For magnetocaloric measurements, magnetization versus magnetic field (M–H) data were recorded at temperatures near Tc, with an applied magnetic field varying from 0 T to 5 T.

3. Results and discussions

The structure and phase purity of $Fe_{1-x}Cu_xCr_2S_4$ (x = 0.0, x = 0.5) were examined using X-ray diffraction (XRD) measurements, and the resulting data were analyzed through Rietveld refinement, as illustrated in Figure 1 (a) and (b). Both compositions crystallize in a cubic spinel structure with the $Fd\bar{3}m$ space group (no. 227), with minor secondary phases identified as Cr_2S_3 for x = 0.0 and $CuCrS_2$ for x = 0.5, respectively. Cr_2S_3 has been reported as a ferrimagnetic material with very weak magnetization below 120 K [19], while $CuCrS_2$ exhibits antiferromagnetic ordering below 40 K [20]. Therefore, we expect these impurities to have a negligible impact on the magnetic and magnetocaloric properties of the samples. The refined structural parameters, including the lattice parameters and R-factors, are summarized in Table 1. The copper substitution for iron is confirmed by a reduction in the cell parameter from 9.9976 to 9.9196 Å in good agreement with the data from Ref. 15. The crystallographic parameters, including atomic positions, isotropic displacement factors, and site occupancies, are provided in Table 2 for both compositions.

Table 1: Refined structural parameters of $Fe_{1-x}Cu_xCr_2S_4$ (x = 0.0, x = 0.5).

Samples	**x = 0.0**	**x = 0.5**
Space groupe	$Fd\bar{3}m$	$Fd\bar{3}m$
Lattice parameter a (Å)	9.9976(1)	9.9196(1)
Unit cell volume V (Å³)	999.28(1)	976.06(1)
R_p (%) **R_{wp} (%)** **R_{exp} (%)**	2.84 3.59 3.37	3.61 4.63 4.17
Chi squared χ^2	1.13	1.23
Bragg R-factor	2.55	4.87
Main phase (Weight %)	96.56(12)	96.24(63)
Impurity (Weight %)	Cr_2S_3 3.44(13)	$CuCrS_2$ 3.76(22)

Table 2: Crystallographic parameters of $Fe_{1-x}Cu_xCr_2S_4$ (x = 0.0, x = 0.5) obtained from Rietveld refinement.

Phase x=0

Atome	Wyckoff symbol	x/a	y/b	z/c	B (Å²)	Occ.
Fe	8b	3/8	3/8	3/8	1.69(8)	0.89(1)
Cr	16c	0	0	0	0.53 (1)	0.94(1)
S	32e	0.24065(8)	0.24065(8)	0.24065(8)	1.21(1)	1.03(1)

Phase x=0.5

Atome	Wyckoff symbol	x/a	y/b	z/c	B (Å²)	Occ.
Fe/Cu	8b	5/8	5/8	5/8	0.93(10)	0.49(5)/0.45(5)
Cr	16c	0	0	0	0.32(7)	0.95(1)
S	32e	0.24187(15)	0.24187(15)	0.24187(15)	0.67(9)	1.03(1)

The scanning electron microscopy (SEM) images and corresponding energy-dispersive X-ray spectroscopy (EDX) analysis of $Fe_{1-x}Cu_xCr_2S_4$ (x = 0.0, 0.5) samples are presented in Figure 2. For the $FeCr_2S_4$ compound (Fig. 2 a), dense agglomerations of particles with varied morphologies are observed, with a particle size of around ten micrometers. The EDX analysis (Fig. 2 c) confirms the presence of Fe, Cr, and S elements, in agreement with the XRD results, thereby validating the elemental composition of the compound. Similarly, the SEM image of the $Fe_{0.5}Cu_{0.5}Cr_2S_4$ compound (Fig. 2 b) shows crystallites with diverse shapes and sizes. The EDX analysis (Fig. 2 d) reveals peaks corresponding to Fe, Cr, S, and additional peaks for copper (Cu), confirming the successful incorporation of Cu into the crystal structure, as supported by the XRD results. The atomic percentages of Fe, Cu, Cr, and S for the $Fe_{1-x}Cu_xCr_2S_4$ (x = 0.0, x = 0.5) samples, determined by EDX, are summarized in Table 3. The experimental data show close agreement with the expected compositions.

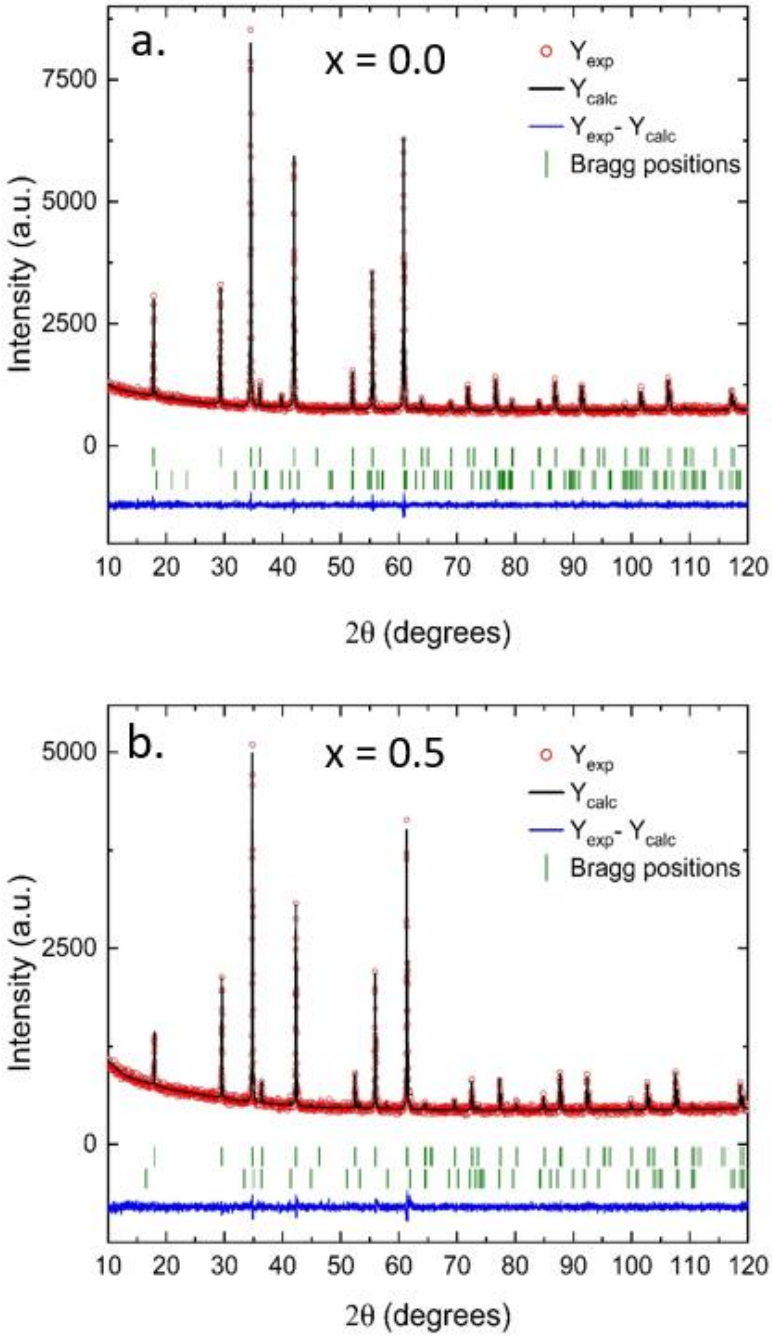

Fig. 1. Rietveld refinement profile of the XRD diagrams of $Fe_{1-x}Cu_xCr_2S_4$ at RT: (a) for x=0.0 and (b) for x=0.5. Red circles and black solid line respectively represent the experimental data (Y_{exp}) and calculated intensity (Y_{calc}). The green solid bars indicate the Bragg peak positions of main phase (first line) and impurity (second line), and the blue curve at the bottom represents the residual (Y_{exp} - Y_{calc}) (difference between experimental and calculated data).

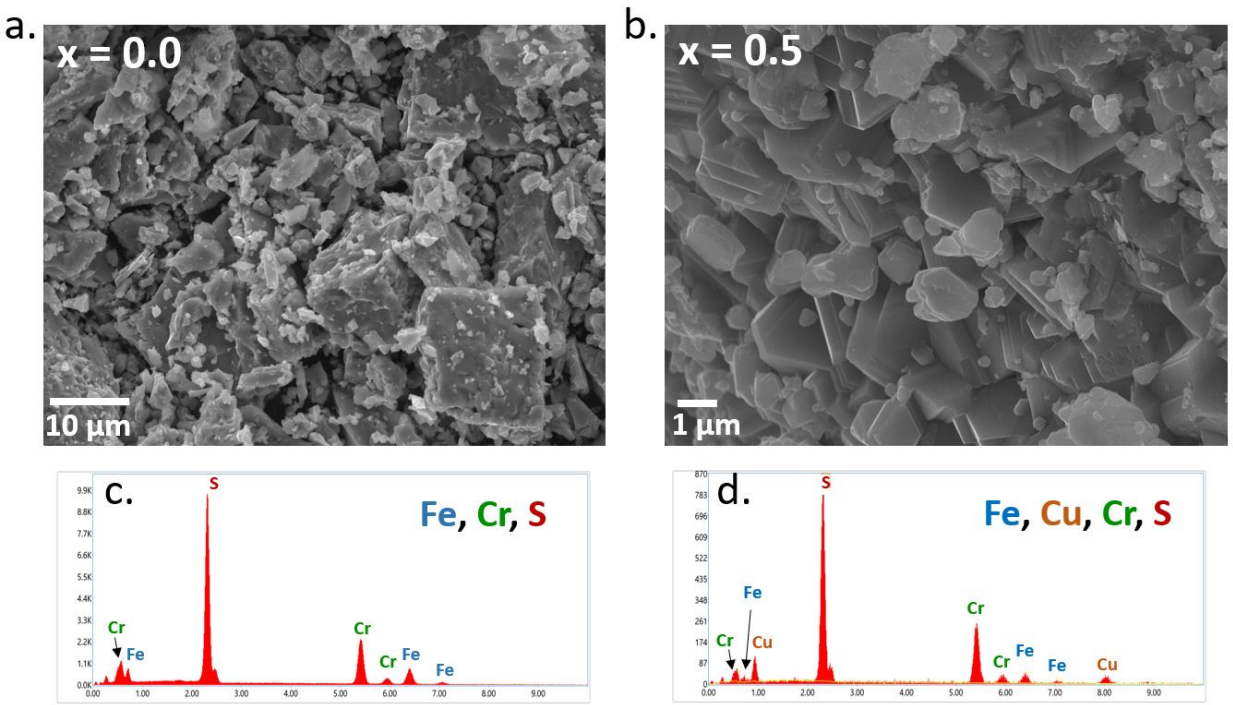

Fig. 2. (a, b) : Typical SEM image and (c, d) the corresponding EDX analysis for our samples.

Table 3: Atomic percentage of Fe, Cu, Cr, and S elements in $Fe_{1-x}Cu_xCr_2S_4$ (x = 0.0, x = 0.5) samples from EDX analyses.

Element	$FeCr_2S_4$ (at. %)	$Fe_{0.5}Cu_{0.5}Cr_2S_4$ (at. %)
Fe	14.80 ± 0.05	7.20 ± 0.12
Cu	-	7.10 ± 0.14
Cr	28.90 ± 0.04	28.01 ± 0.05
S	56.30 ± 0.04	57.69 ± 0.05
Atomic composition :	$Fe_{1.036}Cr_{2.023}S_{3.941}$	$Fe_{0.504}Cu_{0.497}Cr_{1.961}S_{4.038}$

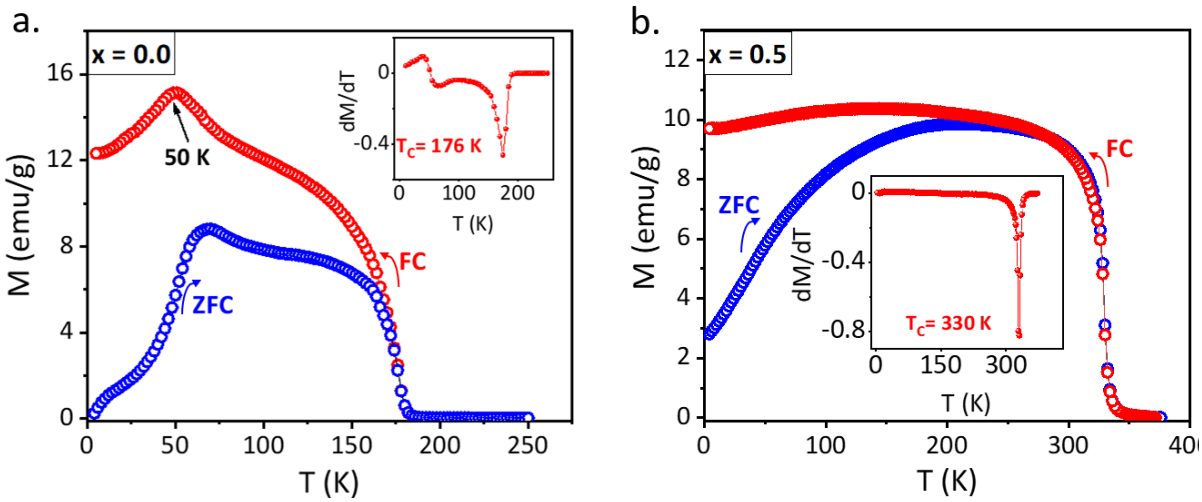

Fig. 3. Temperature dependence of magnetization measured in the ZFC and FC modes in a magnetic induction field of 0.01 T for $Fe_{1-x}Cu_xCr_2S_4$: x = 0.0 (a) and x = 0.5 (b). The insets show plots of dM/dT versus T for both compounds.

The thermal variations of zero-field-cooled (ZFC) and field-cooled (FC) magnetization curves for $Fe_{1-x}Cu_xCr_2S_4$ (x = 0.0, x = 0.5) in a magnetic field of 0.01 T are reported in figure 3. As compared to $FeCr_2S_4$, for which a Curie temperature value T_C = 176 K is found [Fig. 3(a)], an increase of T_C up to 330 K is evidenced for $Fe_{0.5}Cu_{0.5}Cr_2S_4$ [Fig. 3(b)]. The fact that T_C is close to room temperature is particularly interesting for technological applications, especially magnetic refrigeration. This value is in satisfactory agreement with the previously reported transition temperature of 347 K [21] and 340 K [16]. In the case of $FeCr_2S_4$, a cusp-like anomaly around 50 K is found in the FC curve [Fig. 3(a)], which is attributed to the formation of a noncollinear helical spin configuration [17,22,23].

The figure 4 displays M ($\mu_0 H$) at 5 K over the range of $\mu_0 H$ = ±5 T for x = 0.0 and x= 0.5 samples. We observe a similar behavior for both samples with a small hysteresis loop. The magnetization clearly increases with the field and tends to saturate at high fields. The magnetization is higher for the Cu-doped compound, with magnetic saturation values of 36 and 51 emu/g for x = 0.0 and x = 0.5, respectively. The increase in magnetization for the Cu-doped compound (x = 0.5) compared to the undoped compound (x = 0.0) can be explained by the localized features of Fe and Cu 3d band electrons, with an orbital contribution to the total

magnetic moment in this ferrimagnetic system being reduced by the effect of Cu doping, as proposed by Park *et al* [24].

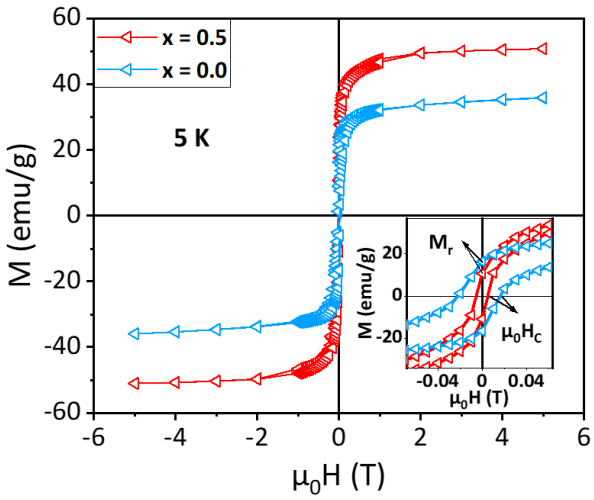

Fig. 4. M-H loops measured at 5 K for the $Fe_{1-x}Cu_xCr_2S_4$ (x = 0.0, x = 0.5) samples.

The insets of Fig. 4 display a zoomed portion of the low magnetic field region. Additionally, we note that our samples have negligible values of remnant magnetizations (M_r) and coercive fields ($\mu_0 H_C$). $\mu_0 H_C$ values were found to be 6×10^{-3} and 5×10^{-3} T for x = 0.0 and x = 0.5, respectively. M_r values were found to be 16.2 and 10.7 emu/g for x = 0.0 and x = 0.5, respectively.

The isothermal magnetization curves of the selected $Fe_{1-x}Cu_xCr_2S_4$ compounds recorded at various temperatures with the applied magnetic field up to 5 T are displayed in Fig. 5. These curves reveal a gradual ferrimagnetic (FiM) to paramagnetic (PM) transition. Below T_C, there is a sharp rise at low magnetic fields, and the magnetization tends to saturate with increasing field, consistent with the typical FiM character observed in both compounds. This behavior arises from the alignment of spins in response to the applied magnetic field. However, above T_C, the magnetization becomes linear, indicating a PM behavior, and decreases with increasing temperature. Arrott-plots (M^2 versus $\mu_0 H/M$) are commonly employed to identify the nature of the magnetic phase transition. According to Banerjee's criteria [25], a magnetic transition is expected to be second-order when the slope of the curve is positive, otherwise the transition will be a first-order. The Arrott plots for the two investigated samples are presented

in Fig. 6. The positive slope in the Arrott plots gives evidence for a second-order magnetic transition for both compounds.

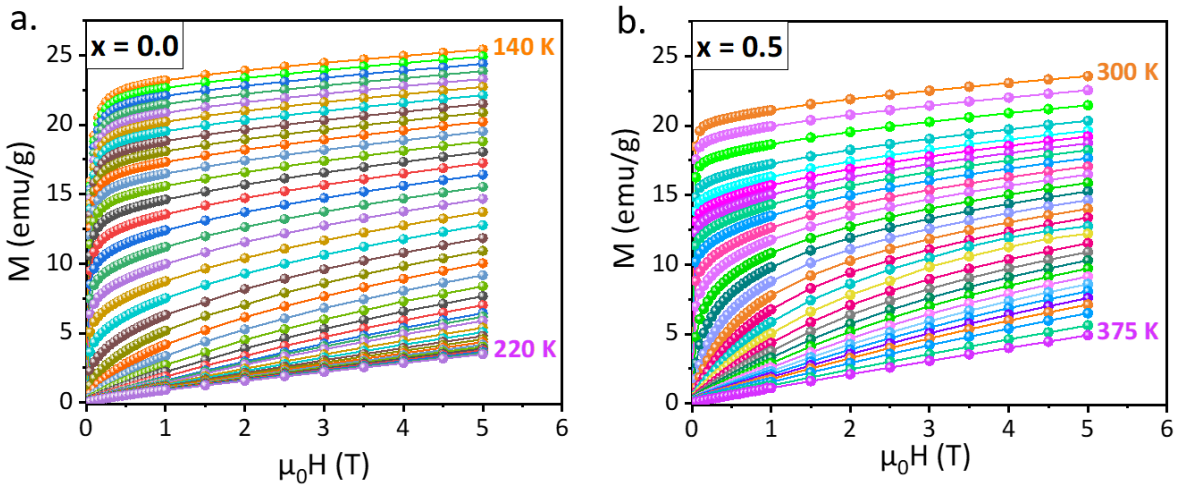

Fig. 5. Isothermal magnetization curves for x = 0.0 (a) and x = 0.5 (b) $Fe_{1-x}Cu_xCr_2S_4$ samples.

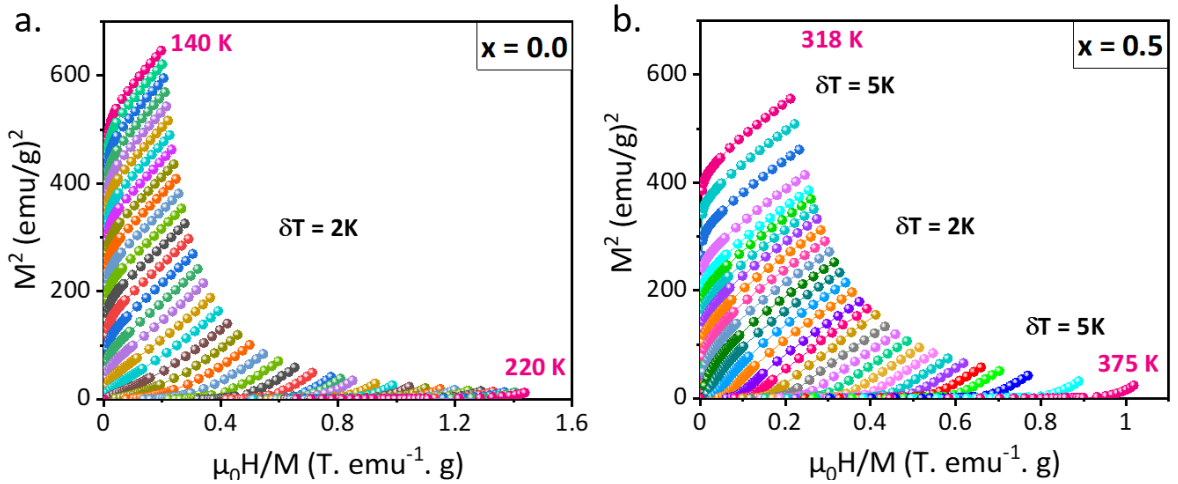

Fig. 6. Arrott plots of for x = 0.0 (a) and x = 0.5 (b) $Fe_{1-x}Cu_xCr_2S_4$ samples at various temperatures.

To investigate the magnetocaloric effect of samples, a series of isothermal magnetic entropy changes were derived from isothermal magnetization experimental data. In accordance with the fundamental principles of thermodynamics, the magnetic entropy change ΔS_M measured in a magnetic field from 0 to H can be expressed as follows:

$$\Delta S_M(T,H) = S_M(T,H) - S_M(T,0) = \int_0^H \left(\frac{\partial S}{\partial H}\right)_T dH \quad (1)$$

Using Maxwell's thermodynamic relation [26]:

$$\left(\frac{\partial S}{\partial H}\right)_T = \left(\frac{\partial M}{\partial T}\right)_H \quad (2)$$

A new formula can be obtained from the last one as follows:

$$\Delta S_M(T,H) = \int_0^H \left(\frac{\partial M}{\partial T}\right)_H dH \quad (3)$$

For magnetization measurements made at discrete field and temperature intervals, the above equation can be approximated by:

$$\Delta S_M(T,H) = \sum \frac{M_{i+1} - M_i}{T_{i+1} - T_i} \Delta H_i \quad (4)$$

Where M_i and M_{i+1} are the experimental magnetization values measured at temperatures T_i and T_{i+1}, respectively, in an external magnetic field H_i. The accuracy of ΔS_M calculated using this method is about 10% [27].

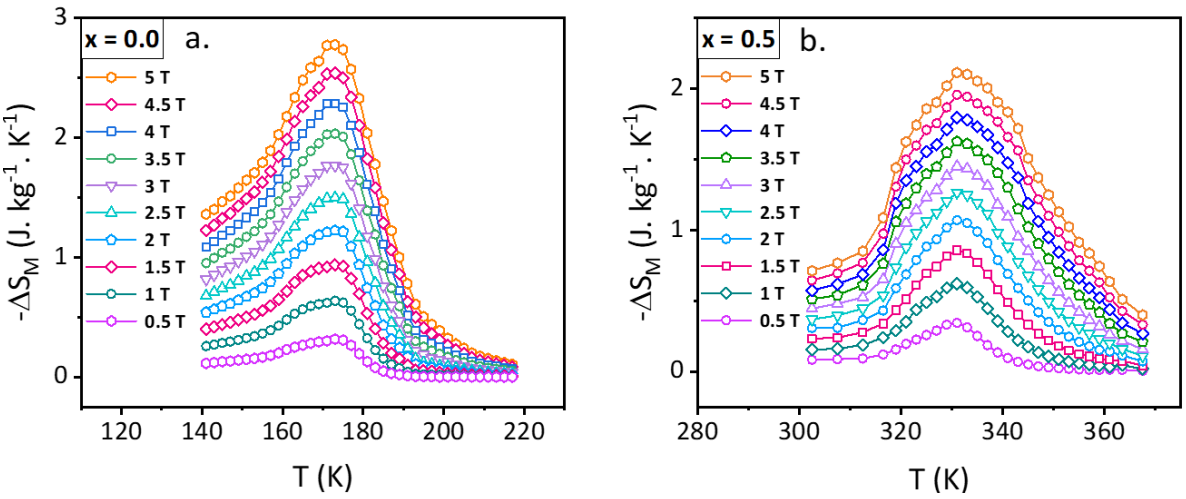

Fig. 7. Magnetic entropy changes ($-\Delta S_M$) versus temperature under different applied magnetic fields for $FeCr_2S_4$ (a) and $Fe_{0.5}Cu_{0.5}Cr_2S_4$ (b).

Figure 7 illustrates the change in magnetic entropy $(-\Delta S_M)$ as a function of temperature for the $Fe_{1-x}Cu_xCr_2S_4$ compounds, calculated at different magnetic fields. The maximum entropy changes for $FeCr_2S_4$ and $Fe_{0.5}Cu_{0.5}Cr_2S_4$ occur near their respective Curie temperatures of 176 K [Fig. 7(a)] and 330 K [Fig. 7(b)]. For $FeCr_2S_4$, we obtained maximum $|\Delta S_M^{max}|$ values of 0.63, 1.77, and 2.78 J/kg. K for ΔH =1, 3, and 5 T, respectively. The latter value is about 33% smaller than that reported by Dey et al. [28], which can be ascribed to a small microstructure difference between the samples influencing magnetic interactions close to T_C.

For the Cu-doped compound, there is a slight reduction in the $|\Delta S_M^{max}|$ values, with corresponding values of 0.62, 1.45, and 2.11 J/kg. K. However, the significant increase in the temperature transition from 176 K for $FeCr_2S_4$ to 330 K for $Fe_{0.5}Cu_{0.5}Cr_2S_4$, is promising for the near room-temperature refrigeration applications.

As shown in Fig. 7, the values of $(-\Delta S_M)$ remain positive throughout the entire temperature range for both compounds, confirming the ferrimagnetic ordering of the Fe-Cr sublattice at T_c. This characteristic behaviour is closely linked to the sign of $\partial M/\partial T$, as described in equation 2. Figure 8 (a) illustrates the variation of the maximum entropy changes $|\Delta S_M^{max}|$ with respect to the magnetic field for $FeCr_2S_4$ and $Fe_{0.5}Cu_{0.5}Cr_2S_4$ compounds. An increase in $|\Delta S_M^{max}|$ is observed with increasing the magnetic applied field for both compounds. A similar trend is observed for the Full Width at Half maximum (FWHM) of the entropy profiles as a function of the applied magnetic field, as shown in figure 8 (b) for both samples.

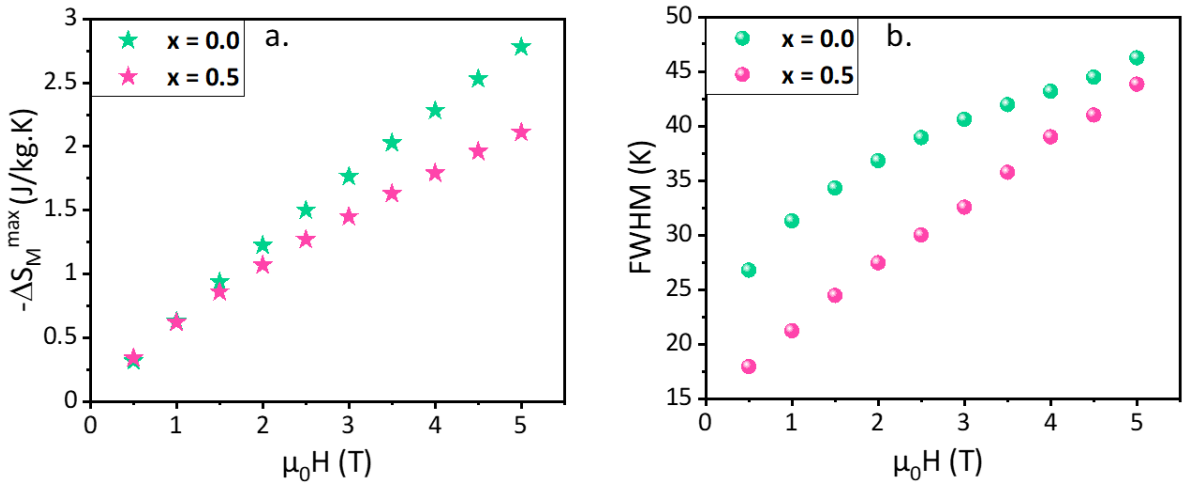

Fig. 8. Magnetic field dependence of (a) the maximum entropy changes and (b) full width at half maximum (FWHM) of the entropy for $FeCr_2S_4$ and $Fe_{0.5}Cu_{0.5}Cr_2S_4$ compounds

The magnetic cooling capability of the material can be related to the relative cooling power (RCP) and the refrigerant capacity (RC), which are commonly used to assess the magnetocaloric material performance. RC and RCP are two interrelated parameters that provide rough estimates of the energy transferred per unit mass between the hot and cold regions during an ideal refrigeration cycle. These parameters can be evaluated using the following equations [2, 29, 30]:

$$\mathrm{RCP} = |\Delta S_M^{max}| \times \delta T_{FWHM} \tag{5}$$

$$\mathrm{RC} = \int_{T_{Cold}}^{T_{Hot}} -\Delta S_M\,(T)\,dT \tag{6}$$

where δT_{FWHM} denotes the full width at half maximum of the magnetic entropy change as a function of temperature, and T_{Cold} and T_{Hot} denote the temperature points at δT_{FWHM}.

The RCP and RC values of $Fe_{1-x}Cu_xCr_2S_4$ (x = 0.0 and x = 0.5) samples around their Curie temperatures are plotted in [Fig. 9(a)] and [Fig. 9(b)], respectively. For both compounds, these parameters follow a monotonous increase with increasing the external magnetic field. For x = 0.0, the RCP and RC values at 5 T are about 128.1 J/kg and 94.0 J/kg, respectively.

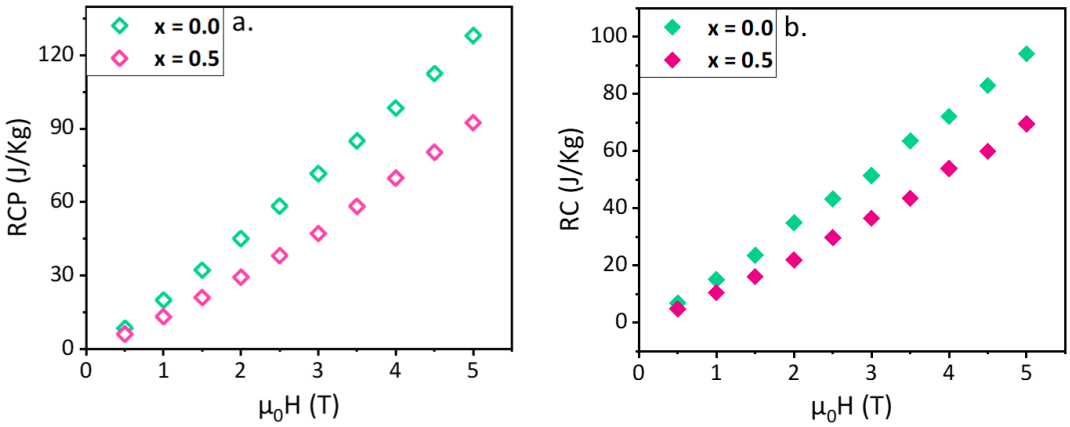

Fig. 9. Relative cooling power (RCP) (a) and refrigerant capacity (RC) (b) versus magnetic field of $Fe_{1-x}Cu_xCr_2S_4$ (x = 0.0, x = 0.5).

Table 4 : Magnetocaloric properties of $Fe_{1-x}Cu_xCr_2S_4$ (x=0.0, x=0.5) compared with previously reported spinel compounds at 5 T.

Compound	T_C (K)	$\lvert\Delta S_M^{max}\rvert$ (J/Kg. K)	RCP (J/Kg)	Reference
$FeCr_2S_4$	176	2.78	128.09	This work
$Fe_{0.5}Cu_{0.5}Cr_2S_4$	330	2.11	92.50	This work
$MnCr_2O_4$	42	5.30	88.17	[31]
$CoCrFeS_4$	312	1.06	51.87	[32]
$CoCr_2O_4$	96	0.76	10.79	[32]
$CoCr_2S_4$	225	3.33	-	[33]
$Co_{0.4}Cu_{0.6}Cr_2S_4$	303	2.57	-	[33]

In comparison, for x = 0.5, the RCP and RC values are found to be 92.5 J/kg and 69.5 J/kg, respectively. The slightly reduced RCP values for the Cu-doped compound as compared to undoped compound are in agreement with the reduced $|\Delta S_M^{max}|$ and FWHM values previously discussed. Also, we found that $RCP \approx 1.3 \times RC$ for both compounds.

To evaluate the magnetocaloric effect performance of our samples, we compared $|\Delta S_M^{max}|$ and RCP values from this study with different magnetic materials having a spinel structure, as reported in Table 4. Given the significantly high magnetic entropy change and relative cooling power values of $Fe_{0.5}Cu_{0.5}Cr_2S_4$, along with its magnetic transition occurring near room temperature, this material presents a promising candidate for magnetic refrigeration applications.

Another important parameter for magnetocalorics is the specific heat change, $\Delta C_P(T,H)$, associated with an applied magnetic field, expressed by the following formula:

$$\Delta C_P(T,H) = C_p(T,H) - C_p(T,0) = T\frac{\partial \Delta S_M(T,H)}{\partial T} \quad (7)$$

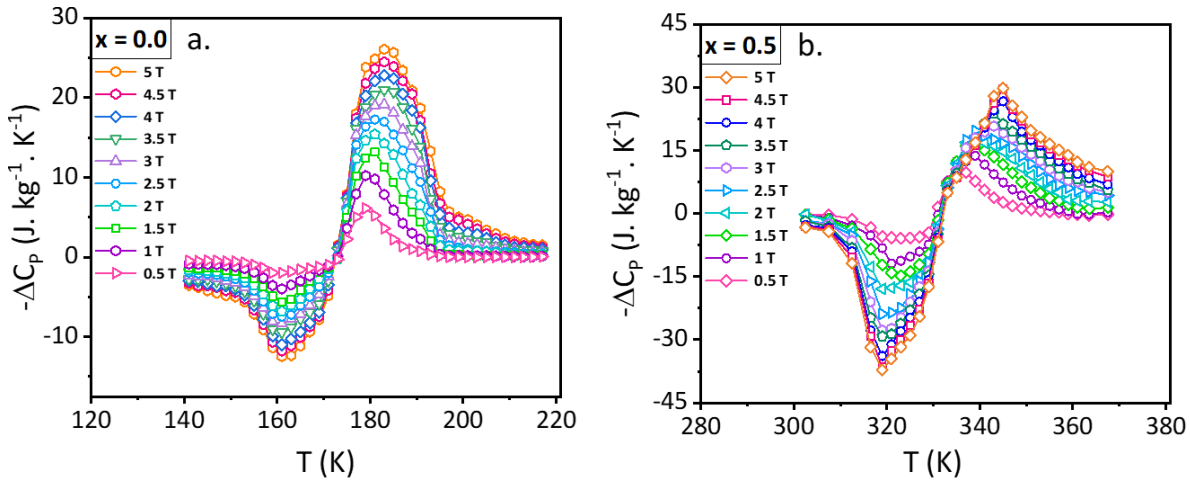

Fig. 10: Specific heat changes ($-\Delta C_P$) under different applied magnetic fields for $FeCr_2S_4$ (a) and $Fe_{0.5}Cu_{0.5}Cr_2S_4$ (b).

Using this equation, we calculated the thermal evaluation of the specific heat change, ΔC_P, for our samples under different field variations, as illustrated in Fig. 10 (a) and (b). Anomalies can be observed in all curves around the critical temperature T_c, transitioning from a negative value below T_c to a positive value above T_c as the temperature increases. Furthermore, the minimum/maximum values of ΔC_P exhibit an increasing trend with the applied magnetic field in the 161 - 183 K and 319 - 345 K ranges for $FeCr_2S_4$ and $Fe_{0.5}Cu_{0.5}Cr_2S_4$, respectively. This suggests that the impact of the magnetic field on the specific heat becomes more pronounced with increasing field strength. Moreover, under a magnetic induction field of 5 T, the amplitude of ΔC_P evolves from 38.6 to 67 J/kg.K when half of Fe is substituted by Cu in the thiospinel compound.

We use a criterion developed by Franco and Conde [34] to ascertain the nature of the magnetic order transition which is based on rescaled entropy change curves for different applied fields. In order to construct the universal curves, it is necessary to normalize the $\Delta S_M(T)$ obtained at different fields to their maximum values $|\Delta S_M^{max}|$, and rescale the temperature axis. Figure 11 (a) and (b) illustrate the construction of universal curves for our samples by plotting $\Delta S'$ against θ, where $\Delta S' = \Delta S_M(T)/|\Delta S_M^{max}|$ and θ represents the new parameter of the temperature axis defined as:

$$\theta = -\frac{T - T_c}{T_{r1} - T_c}, T \leq T_c \; ; \;\; \theta = \frac{T - T_c}{T_{r2} - T_c}, T > T_c \tag{8}$$

where T_{r1} and T_{r2} are the two reference temperatures. In our case, they are chosen in a way that $\Delta S_M(T_{r1}) = \Delta S_M(T_{r2}) = 0.5\ |\Delta S_M^{max}|$.

If the phenomenological universal curves converge onto a single curve under different applied fields, it indicates that the compound undergoes a second order ferrimagnetic phase transition [35, 36]. Conversely, if the universal curve does not collapse into a single curve, it suggests a first-order magnetic phase transition. As shown in Fig. 11, there is a clear collapse of normalized curves under different magnetic fields for $FeCr_2S_4$ and $Fe_{0.5}Cu_{0.5}Cr_2S_4$, respectively. This result gives evidence for a second order phase transition occurring in our samples, in agreement with the Arrott plots constructions shown in Fig. 6.

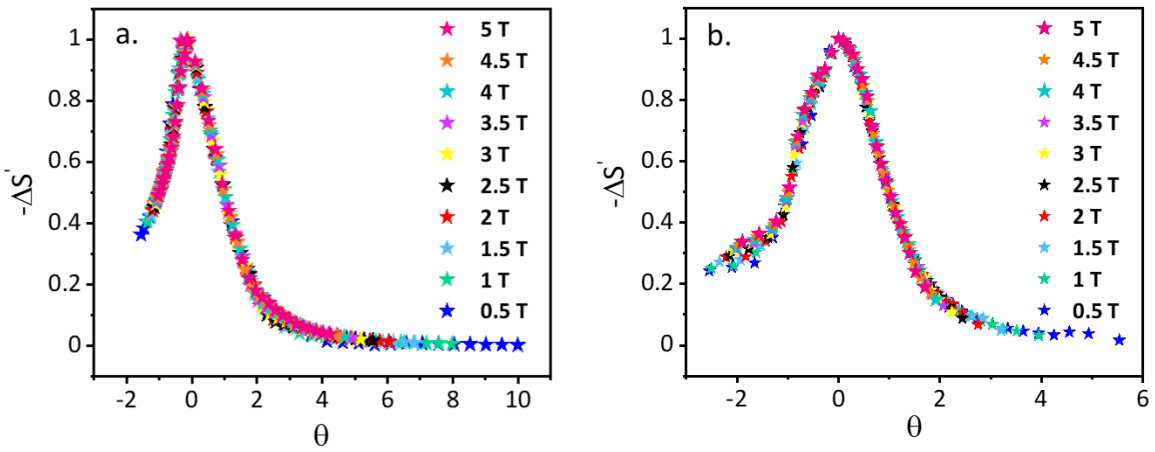

Fig. 11 . Universal curve of the scaled entropy changes for (a) $FeCr_2S_4$ and (b) $Fe_{0.5}Cu_{0.5}Cr_2S_4$ at different applied magnetic field changes.

4. Conclusions

In summary, we studied the magnetic and magnetocaloric properties of $FeCr_2S_4$ and $Fe_{0.5}Cu_{0.5}Cr_2S_4$ spinel compounds. The magnetic entropy changes ΔS_M were calculated using isothermal magnetization curves around the magnetic transition temperatures of each material. Under a 5 T magnetic field, the maximum magnetic entropy changes were found to be 2.78 J/kg. K for $FeCr_2S_4$ and 2.11 J/kg. K for $Fe_{0.5}Cu_{0.5}Cr_2S_4$. The relative cooling power (RCP)

values decreased slightly with Cu substitution, yet remained promising. Specifically, the RCP for $FeCr_2S_4$ was 128.09 J/Kg and for $Fe_{0.5}Cu_{0.5}Cr_2S_4$ it was 92.5 J/Kg under 5 T magnetic field. These findings indicate that $Fe_{0.5}Cu_{0.5}Cr_2S_4$ could be a promising material for magnetic refrigeration applications due to its temperature transition near room temperature, substantial magnetic entropy change, and high relative cooling power compared to other materials with spinel structure.

CRediT authorship contribution statement

J.J., A.F., and S.H. conceived and supervised the study. S.E.H. elaborated the powders and carried out with D. P. the structural characterizations. E.C and F.R. performed the magnetic measurements and data analysis. E.C wrote the manuscript which was reviewed by all authors. All authors discussed the data and contributed to analysis and feedback.

Data availability

The data that support the findings of this study are available from the corresponding author upon reasonable request.

Acknowledgments

The authors acknowledge the financial support from LabEx EMC3 (Excellence Laboratory, Grant No. 10-LABX-0009) of the French National Research Agency (ANR) through the SPINTEP project, the support of the CNRS Research Foundation IRMA (FR 3095), the support of the Agence Nationale de la Recherche under Grant ANR-21-CE50-0033, and the support received from the Normandy Region (Réseau d'Intérêt Normand - Label d'excellence).

References

[1] E. Brück, « Developments in magnetocaloric refrigeration », *J. Phys. Appl. Phys.*, vol. 38, n° 23, p. R381-R391, 2005, doi: 10.1088/0022-3727/38/23/R01.

[2] V. Franco, J. S. Blázquez, J. J. Ipus, J. Y. Law, L. M. Moreno-Ramírez, and A. Conde, "Magnetocaloric effect: From materials research to refrigeration devices", *Prog. Mater. Sci.*, vol. 93, p. 112-232, 2018, doi: 10.1016/j.pmatsci.2017.10.005.

[3] V. K. Pecharsky and K. A. Gschneidner, Jr., « Giant Magnetocaloric Effect in Gd5(Si2Ge2) », *Phys. Rev. Lett.*, vol. 78, n° 23, p. 4494-4497, 1997, doi: 10.1103/PhysRevLett.78.4494.

[4] L. Morellon, J. Blasco, P. A. Algarabel, and M. R. Ibarra, "Nature of the first-order antiferromagnetic-ferromagnetic transition in the Ge-rich magnetocaloric compounds $Gd_5(Si_xGe_{1-x})_{4''}$, *Phys. Rev. B*, vol. 62, n° 2, p. 1022-1026, 2000, doi: 10.1103/PhysRevB.62.1022.

[5] F. Hu, B. Shen, J. Sun, Z. Cheng, G. Rao, and X. Zhang, "Influence of negative lattice expansion and metamagnetic transition on magnetic entropy change in the compound LaFe11.4Si1.6", *Appl. Phys. Lett.*, vol. 78, n° 23, p. 3675-3677, 2001, doi: 10.1063/1.1375836.

[6] F. Guillou, G. Porcari, H. Yibole, N. van Dijk, and E. Brück, "Taming the First-Order Transition in Giant Magnetocaloric Materials", *Adv. Mater.*, vol. 26, n° 17, p. 2671-2675, 2014, doi: 10.1002/adma.201304788.

[7] L. Li, K. Nishimura, W. D. Hutchison, Z. Qian, D. Huo, and T. NamiKi, "Giant reversible magnetocaloric effect in ErMn2Si2 compound with a second order magnetic phase transition", *Appl. Phys. Lett.*, vol. 100, n° 15, p. 152403, 2012, doi: 10.1063/1.4704155.

[8] J. Shen, J.-F. Wu, and J.-R. Sun, "Room-temperature large refrigerant capacity of $Gd_6Co_2Si_3$", *J. Appl. Phys.*, vol. 106, n° 8, p. 083902, 2009, doi: 10.1063/1.3243289.

[9] G. Alouhmy, R. Moubah, E. H. Sayouty, and H. Lassri, "Comparative studies of magnetic and magnetocaloric properties in amorphous Gd0.67Y0.33 and Gd0.67Zr0.33 films", *Solid State Commun.*, vol. 250, p. 14-17, 2017, doi: 10.1016/j.ssc.2016.11.009.

[10] A. P. Ramirez, R. J. Cava and J. Krajewski, "Colossal magnetoresistance in Cr-based chalcogenide spinels", *Nature* 386 p. 156, 1997, doi: 10.1038/386156a0.

[11] V. Tsurkan *et al.*, “Structural anomalies and the orbital ground state in FeCr 2 S 4”, *Phys. Rev. B*, vol. 81, nº 18, p. 184426, 2010, doi: 10.1103/PhysRevB.81.184426.

[12] D. Maurer, V. Tsurkan, S. Horn, and R. Tidecks, “Ultrasonic study of ferrimagnetic FeCr2S4: Evidence for low temperature structural transformations”, *J. Appl. Phys.*, vol. 93, nº 11, p. 9173-9176, 2003, doi: 10.1063/1.1570930.

[13] M. Ito *et al.*, “Magnetic properties of spinel FeCr2S4 in high magnetic field”, *J. Magn. Magn. Mater.*, vol. 323, nº 24, p. 3290-3293, 2011, doi: 10.1016/j.jmmm.2011.07.041.

[14] G. Haacke and L. C. Beegle, “Magnetic properties of the spinel system Fe1−xCuxCr2S4”, *J. Phys. Chem. Solids*, vol. 28, nº 9, p. 1699-1704, 1967, doi: 10.1016/0022-3697(67)90144-8.

[15] V. Tsurkan *et al.*, “Influence of cation substitution on the magnetic properties of the FeCr2S4 ferrimagnet”, *J. Phys. Chem. Solids*, vol. 66, nº 11, p. 2040-2043, 2005, doi: 10.1016/j.jpcs.2005.09.040.

[16] Z. Klencsár *et al.*, “Mössbauer study of Cr-based chalcogenide spinels Fe1−xCuxCr2S4”, *Phys. B Condens. Matter*, vol. 358, nº 1-4, p. 93-102, 2005, doi: 10.1016/j.physb.2004.12.033.

[17] G. M. Kalvius *et al.*, “Magnetism of the chromium thio-spinels $Fe_{1-x}Cu_xCr_2S_4$ studied using muon spin rotation and relaxation” *J. Phys. Condens. Matter*, vol. 25, nº 18, p. 186001, 2013, doi: 10.1088/0953-8984/25/18/186001.

[18] a Windows tool for powder diffraction patterns analysis. *T. Roisnel, J. Rodriguez-Carvajal.* Materials Science Forum, Proceedings of the Seventh European Powder Diffraction Conference (EPDIC 7), 2000, p.118-123, Ed. *R. Delhez and E.J. Mittenmeijer.*

[19] Bertautt et al., ‘’ Etude de Cr2S3 rhomboedrique par diffraction neutronique et mesures magnétiques’’, Journal of physique, vol. 29, n 8-9, p.813-824, 1968 **,** doi :10.1051/jphys:01968002908-9081300.

[20] Le Nagard et al. , ‘’Etude structurale et proprietes physiques de CuCrS2 ’’, Materials Research Bulletin, V. 14, n. 11, P . 1411-1417, 1979 , doi : 10.1016/0025-5408(79)90083-7.

[21] G. M. Kalvius *et al.*, "Spin-lattice instability in the chromium sulfur spinel $Fe_{0.5}Cu_{0.5}Cr_2S_4$", *J. Phys. Condens. Matter*, vol. 20, nº 25, p. 252204, 2008, doi: 10.1088/0953-8984/20/25/252204.

[22] G. M. Kalvius *et al.*, "Low temperature incommensurately modulated and noncollinear spin structure in $FeCr_2S_4$", *J. Phys. Condens. Matter*, vol. 22, nº 5, p. 052205, 2010, doi: 10.1088/0953-8984/22/5/052205.

[23] J. Engelke *et al.*, "Spin re-orientation in FeCr2S4", *Hyperfine Interact.*, vol. 202, nº 1-3, p. 57-61, nov. 2011, doi: 10.1007/s10751-011-0338-0.

[24] Min Sik Park *et al.*, "Half-metallic electronic structures of giant magnetoresistive spinels: Fe 1- x Cu x Cr 2 S 4 (x= 0.0, 0.5, 1.0)", Physical Review B, vol. 59, p.10018, April 1999, doi: 10.1103/PhysRevB.59.10018

[25] B. K. Banerjee, "On a generalised approach to first and second order magnetic transitions", *Phys. Lett.*, vol. 12, nº 1, p. 16-17, sept. 1964, doi: 10.1016/0031-9163(64)91158-8.

[26] T. Hashimoto, T. Numasawa, M. Shino, and T. Okada, "Magnetic refrigeration in the temperature range from 10 K to room temperature: the ferromagnetic refrigerants", *Cryogenics*, vol. 21, nº 11, p. 647-653, nov. 1981, doi: 10.1016/0011-2275(81)90254-X.

[27] V. K. Pecharsky and K. A. Gschneidner, "Magnetocaloric effect from indirect measurements: Magnetization and heat capacity", *J. Appl. Phys.*, vol. 86, nº 1, p. 565-575, juill. 1999, doi: 10.1063/1.370767.

[28] K. Dey *et al.*, "Multicaloric effect in multiferroic sulpho spinel MCr2S4 (M = Fe & Co)". *J. Magn. Magn. Mater.* 498 (2020) 166090, doi :10.1016/j.jmmm.2019.166090.

[29] T. M. Al-Shahumi, I. A. Al-Omari, S. H. Al-Harthi, and M. T. Z. Myint, "Synthesis, structure, morphology, magnetism, and magnetocaloric-effect studies of (La1−xPrx)0.7Sr0.3MnO3 nanocrystalline perovskites", *SN Appl. Sci.*, vol. 5, nº 4, p. 121, avr. 2023, doi: 10.1007/s42452-023-05328-5.

[30] M. Bouhbou, R. Moubah, W. Belayachi, A. Belayachi, L. Bessais, and H. Lassri, "Magnetic and magnetocaloric properties in sulfospinel Cd1−Zn Cr2S4 (x= 0, 0.3, 0.5) powders", *Chem. Phys. Lett.*, vol. 688, p. 84-88, nov. 2017, doi: 10.1016/j.cplett.2017.09.059.

[31] K. Dey, A. Indra, S. Majumdar, and S. Giri, “Critical behavior and reversible magnetocaloric effect in multiferroic MnCr 2 O 4”, *J. Magn. Magn. Mater.*, vol. 435, p. 15-20, août 2017, doi: 10.1016/j.jmmm.2017.03.068.

[32] S. Gulkesen, K. U. Tumen, M. Akyol, and A. Ekicibil, “Room-temperature magnetocaloric effect in Fe-substituted CoCr2O4 spinels”, *Appl. Phys. A*, vol. 127, n° 3, p. 211, mars 2021, doi: 10.1007/s00339-021-04374-3.

[33] X.-C. Zheng, X.-Y. Li, L.-H. He, S.-Y. Zhang, M.-H. Tang, and F.-W. Wang, “Magnetic properties and magnetocaloric effect of the Cr-based spinel sulfides $Co_{1-x}Cu_xCr_2S_4$”, *Chin. Phys. B*, vol. 26, n° 3, p. 037502, 2017, doi: 10.1088/1674-1056/26/3/037502.

[34] V. Franco and A. Conde, “Scaling laws for the magnetocaloric effect in second order phase transitions: From physics to applications for the characterization of materials”, *Int. J. Refrig.*, vol. 33, n° 3, p. 465-473, 2010, doi: 10.1016/j.ijrefrig.2009.12.019.

[35] B. Sattibabu, A. K. Bhatnagar, K. Vinod, A. Mani, and D. Das, “Large magnetocaloric effect in hexagonal Yb1−xHoxMnO3”, *Appl. Phys. Lett.*, vol. 107, n° 26, p. 262904, 2015, doi: 10.1063/1.4938750.

[36] N. Kumar Swamy *et al.*, “Specific heat and magnetocaloric effect studies in multiferroic YMnO3”, *J. Therm. Anal. Calorim.*, 119, p. 1191-1198, (2015), doi: 10.1007/s10973-014-4223-3.